Chapter 11
Time-of-Flight Spectroscopy

Tetsuya Inagaki and Satoru Tsuchikawa

Abstract This chapter summarizes the principle and application of time-of-flight (TOF) NIR spectroscopy, which can evaluate the contribution of scattering and absorption of light in samples simultaneously. In order to construct robust calibrations for organic materials by NIR spectroscopy, it is important to evaluate and understand the spectral contribution from light absorption (absorption resulting from harmonics or overtones of the fundamental absorptions of molecular vibrations) and light scattering (mainly due to the cellular structure). In this chapter, we introduce the principle of TOF-NIR spectroscopy and some applications to agricultural, medical area, and forest products.

Keywords Time-resolved spectroscopy · Time-of-flight spectroscopy · Spatially resolved spectroscopy · Absorption coefficient · Reduced scattering coefficient

11.1 Introduction

In the past three decades, many researchers have paid attention to the potential use of NIR spectroscopy as a practical use for the detection of organic compounds in materials. In fields such as agriculture, food, pharmaceuticals, medical, paper, and polymers, there is a strong interest in NIR spectroscopy because of its nondestructiveness, accuracy, quick measurement, and easy operation. The measurement of NIR spectra (i.e., detection of NIR light from the sample) is done by transmittance (including interactance) or diffuse reflectance mode. The transmission method is desirable for detecting internal information in large quantities of material, although the optical information from the diffuse reflectance spectrum is limited to the surface of the sample. It is particularly important to proceed with the development of NIR transmission devices for detecting the internal properties of high moisture fruits, vegetable products, or thick wood products.

T. Inagaki (✉) · S. Tsuchikawa
Graduate School of Bioagricultural Sciences, Nagoya University, Nagoya, Japan
e-mail: inatetsu@agr.nagoya-u.ac.jp

Y. Ozaki et al. (eds.), *Near-Infrared Spectroscopy*,
https://doi.org/10.1007/978-981-15-8648-4_11

Behavior of transmitted or diffuse reflected light from an agricultural, forest product or human body (i.e., highly scattering media) is strongly affected by both physical and chemical properties of the tissues, making it complicate to examine the optical characteristics of the tissue in detail and to evaluate the sample constituents accurately. Especially in the 500–1100 nm wavelength range for most biological media, the scattering coefficient is much higher than the absorption coefficient. Although many studies have reported that the chemical, physical, and mechanical properties of biological material can be predicted by NIR diffuse reflectance/transmittance spectroscopy with the aid of statistical methods (i.e., chemometrics), such chemometric NIR approaches have some disadvantages. First, the contribution of the light absorption and scattering phenomena in acquired spectra cannot be explained independently. Second, the construction of a calibration model, which is usually not transferable among instruments, requires a considerable amount of spectral and objective data. Additionally, the light scattering contribution to NIR spectra is significant when the material has complex cellular structure result in the high scattering of light. In order to construct robust calibrations for organic materials by NIR spectroscopy, it is of importance to independently evaluate the spectral contribution from light absorption (absorption resulting from harmonics or overtones of the fundamental absorptions of molecular vibrations) and light scattering (mainly due to the cellular structure and refractive index mismatch at the boundary).

In order to understand such a complex phenomena of light propagation in organic materials, many researchers have given attention to time-of-flight (TOF) or time-resolved (TR) spectroscopy using short pulses of light emission and observe the reflected or transmitted light as a function of time in nano or pico order. A time-resolved measurement, or time domain system, could provide the TOF information of the detected light. In the TOF approach, tens of picosecond light pulses are usually injected into the tissue, usually using a suitable optical fiber.

The intensity of light pulse propagates through the tissue is detected at a certain distance from the injection point (Fig. 11.1). It is also possible to examine biological tissue using the transmission approach. In this approach, the source and detector fibers are placed on opposite sides of the tissue. Time domain intensity of photons propagated into the tissue, known as the photon distribution of time of flight (DTOF), results delayed, broadened, and attenuated because of the scattering and absorption of light inside the diffusive medium. Although it is possible to estimate the optical properties of materials by spatially resolved technique (SR) or spatial frequency domain technique, it is considered that TR technique is more accurate in the measuring of optical properties.

Patterson et al. [1] proposed the usefulness of the time-resolved reflectance and transmittance spectroscopy for the noninvasive measurement of tissue optical properties theoretically. They developed a model based on the diffusion approximation of radiative transfer, which yielded an analytical expression for pulse shape in terms of the interaction with a homogeneous slab, for the determination of optical properties [i.e., absorption coefficient (μ_a) and reduced scattering coefficient (μ_s')] in tissue. μ_s' is defined as

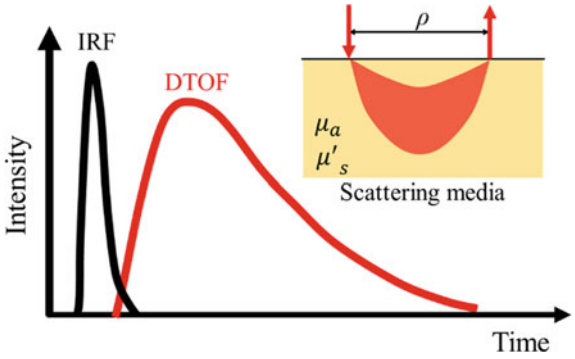

Fig. 11.1 Summary of TR NIR spectroscopy. The injected pulse (IRF: instruments response function) propagate into scattering media with absorption coefficient and reduced scattering coefficient. The detected light intensity at certain distance from injected point (ρ) with time domain broadens due to light scattering (DTOF: distribution of time-of-flight)

$$\mu_s' = (1 - g)\mu_s$$

where μ_s is the linear scattering coefficient, and g is the mean cosine of the scattering angle. A value of $g = 1$ represents forward scattering, while $g = 0$ represents isotropic scattering. Under the assumption that $\mu_a \ll \mu_s'$ (i.e., high scattering media), the diffusion of a photon can be considered to be in a random walk of step size $1/\mu_s'$, where each step involves isotropic scattering. Patterson et al. solve the diffusion equation using Green's function with two assumptions; 1. All the incident photon are initially scattered at the depth of $z_0 = 1/\mu_s'$ and 2. diffuse photon rate at the physical boundary between tissue and non-scattering medium would be 0. They successfully express the reflectance and transmittance ratio with the function of distance from light source and time. The usefulness of the function they reported has been proven by many researches. However, Leonardi and Burns [2] investigated quantitative measurements in scattering media on the basis of TOF spectroscopy with analytical descriptors. They found that experimental analysis from time-resolved profiles is efficient in estimating absorption and scattering coefficients. Numerical methods such as adding-doubling and Monte Carlo (MC) methods simulating light propagation in biological tissues are also often used.

Many researches revealed that the determination of μ_a and μ_s' in agricultural and food products can be used for the evaluation of chemical and physical properties in samples [3–5]. In the field of medical science, time domain method is expected to develop optical tomography techniques, which can be used for the noninvasive detection of cancer [6] or the changes of hemoglobin concentration associated with neural activation in human brain [7]. In this chapter, we introduce the principle of TOF-NIR spectroscopy and some applications to agricultural, medical area and forest products.

11.2 Measuring Apparatus

For the detection of DTOF data of samples, measuring system should contain 1. laser source, 2. photodetector, and 3. time-resolved system. Torricelli et al. summarized [4] the evolution history of TR spectroscopic components, i.e., in the first generation since the early 1990s, the laser from gas, dye, or solid state laser was used as light source and detected DTOF profiles using microchannel plate photomultiplier (PMT) with electronic chain for time-correlated single photon counting (TCSPC) with NIM module. The TR spectroscopic components at the second generation, 2000–2010, semiconductor laser heads with external RF driver was used as light source and detected by compact metal channel dynode PMT with TCSPC electronic board system. Now it is possible to use the supercontinuum fiber laser with powerful emission with broad wavelength range as light source and detected by hybrid PMT with time-to-digital converters module with USB controller. The distance from light injection points to receiver (ρ in Fig. 11.1) should be optimized according to the range of μ_a and μ_s' of the samples. Estimated value of attenuation is in the order of 10^6–10^8, and temporal dynamic span is over a 1–10 nm range when the sample has general optical properties in the NIR region, i.e., $\mu_a = 0 - 0.05\ \text{cm}^{-1}$, $\mu_s' = 5 - 25\,\text{cm}^{-1}$ and $\rho = 1 - 3$ cm.

11.3 Data Analysis

After obtaining the time-resolved light intensity signal, μ_a and μ_s' are estimated by fitting the TR data obtained with the analytical solution of the diffusion equation by the nonlinear inverse algorithm. Convolution between the theoretical TR reflectance with the IRF is calculated at first in order to take the broad shape of the IRF and then used to fit the experimental TR reflectance curve. As mentioned in introduction, solution of diffusion equation can be applied only if the scattering is dominant compared to absorption in media, and radiance is detected at a sufficient larger distance from the injection point, i.e., distance should be much longer than one mean free path $1/\mu'$. MC simulation is also used to model the light propagation in biological tissue because of its flexibility and simplicity to simulate photon propagation processes in arbitrary shapes with complex boundary conditions or spatial localization. For that simulation, the photon propagation in the turbid medium is traced until it exits the sample surface or is absorbed. The movement of photons from one photon tissue interaction to the next photon tissue interaction is described by a probability function using the optical properties of the tissue. Repeat these processes for a large number of photons to estimate the photon distribution in the tissue. Detailed explanation for the data analysis with fitting or MC simulation can be found in book [8].

11.4 Application of TOF-NIRS to Agricultural Science

The important parameters for fruits or vegetables (i.e., maturity, quality parameters, and defect) can be detected by measuring the optical parameters as Lu et al. reviewed [5]. The couple of most important quality attributes to different fruits are firmness and soluble solids content (SSC). Many studies demonstrate that both μ_a and μ_s' have relation to hardness, SSC, and skin color. However, it was generally reported that μ_a was suitable for predicting these quality parameters. This may be due to the fact that pigments or other chemical compositions would change during maturation with changes of cell structure directly affecting hardness. In most of the cases, the combination of μ_a and μ_s' was found to improve the prediction of fruit maturity and quality parameters. The prediction of firmness and SSC by TR technology was widely reported for apple, kiwifruit, mango, nectarine, peach, and pear. Because physiological disorders often cause the changes in the chemical and structural properties of the fruits product result in the change of μ_a and μ_s', it is possible to detect the defect in the fruits by observing the optical properties in fruits. Especially, TR technology can be used to detect internal browning and internal bleeding of apples, nectarines, plums, thanks to its ability to penetrate tissue deeper inside the fruits. Determined bulked absorption coefficients of fruits in the spectral regions of 500–1850 nm were largely dominated by the water in the NIR range and fruit-specific pigments in the visible range. The differences in μ_s' behavior (μ_s'decrease exponentially with the increase of wavelength) between fruits, cultivars and tissue type are related to microstructural differences, such as differences in cellular structure and porosity. μ_s'values are reported for various fruits ranging from 0 to 20 cm^{-1}.

11.5 Application of TOF-NIRS to Medical Science

One of the research areas where TR investigation is most actively conducted is the medical science. Diffuse optical tomography in NIR region at the range of wavelength from 700 to 1000 nm is proven to have the potential for noninvasive diagnoses of tissue oxygenation and thyroid cancers. As a first step toward properly designing devices, interpreting diagnostic measurements or planning therapeutic is to identify the accurate optical properties of a tissue. Following research might be the use of optical properties determined to describe the light transportation and absorption. Jacques [9] summarized 1. μ_a of various tissues in terms of the average hemoglobin concentration or some similar properties and 2. μ_s' with the parameters (a, b), or alternatively (a', f_{Rayleigh}, b_{Mie}) which explain the μ_s' variation with wavelength change. The $\mu_s'(\lambda)$ were expressed by the equation $\mu_s' = a\left(\frac{\lambda}{500(\text{nm})}\right)^{-b}$ or $\mu_s' = a'\left(f_{\text{Rayleigh}}\left(\frac{\lambda}{500(\text{nm})}\right)^{-4} + \left(1 - f_{\text{Rayleigh}}\right)\left(\frac{\lambda}{500(\text{nm})}\right)^{-b_{\text{Mie}}}\right)$ where the λ is wavelength. In the later equation, scattering is described in terms of the separate contribution

of Rayleigh and Mie scattering. Author explained that the equations are good for use in predicting behavior of light propagation or diffusion within the 400–1300 nm wavelength range. Author summarized also the mean values of coefficient a and b (skin: $a = 46.0\ \mathrm{cm}^{-1}$, $b = 1.421$, brain: $a = 24.2\ \mathrm{cm}^{-1}$, $b = 1.611$, breast: $a = 16.8\ \mathrm{cm}^{-1}$, $b = 1.055$, bone: $a = 22.9\ \mathrm{cm}^{-1}$, $b = 0.716$, other soft tissues: $a = 18.9\ \mathrm{cm}^{-1}$, $b = 1.286$, other fibrous tissues: $a = 27.1\ \mathrm{cm}^{-1}$, $b = 1.627$, fatty tissue: $a = 18.4\ \mathrm{cm}^{-1}$, $b = 0.672$). Fujii et al. [6] investigated the effects of three factors (trachea, refractive index mismatch at the boundary of trachea tissue, and neck organs other than the trachea [spine, spinal cord, and blood vessels]) on light propagation in the neck by 2D time-dependent radiative transfer equation. After they constructed an anatomical model of human neck from MR image, they performed segmentation of the MR image and recognized the pixel corresponding to organs of the human neck: the trachea, spine, spinal cord, and blood vessels. They simulated the light propagation in anatomical human neck models by numerical method and MC simulation. They showed that reflection and refraction at the trachea tissue interface significantly effect on the light intensities in the region between the trachea and the front of the neck surface. So, it is necessary to take into account the refractive index mismatch at the trachea tissue interface. Hoshi summarized the use of TR system for clinical monitoring of tissue oxygenation [7].

11.6 Application of TOF-NIRS to Forest Products

As many reviews and manuscripts about application of TR spectroscopy for medical and food product science are published, TR spectroscopic application for these research area is briefly explained in previous chapter. In present chapter, the use of TR spectroscopy for the determination of optical properties in wood is explained in detail.

Wood is a natural material widely used in construction because of its versatility and strength. As wood is a biomaterial, there are significant variations in wood properties (e.g., density, moisture content, grain angle) between species and even among the same species. From the point of view of quality assurance in industry, nondestructive measuring and control of the mechanical, physical, and chemical properties of wood are strongly desired. The light scattering in wood is especially complex because of the complex cellular structure in wood. Softwood mainly possesses a tracheid structure, arrayed along the longitudinal direction; whereas, hardwood structures have wide variation of cell structure (e.g., tracheids, vessels, libriform wood fibers, or ray cells). The optical properties of wood are significantly affected also by the water retained in cell walls or cell lumens.

Some groups reported the use of TR diffuse reflectance spectroscopy to determine the optical properties of wood. D'Andrea et al. [10] decided μ_a and μ_s' in the wavelength range of 700–1040 nm of two wood species treated in different conditions (dry wood, wet wood, and degraded wood) by TR spectroscopy with two orientations of the optical fiber (i.e., the emitted and detected fibers

are set perpendicular or parallel to wood grain orientation) and obtained many interesting results. They reported that the μ_s' (10–200 cm^{-1}) was much larger than the μ_a (0.05–1.00 cm^{-1}) for all wood samples. μ_s' spectra were almost constant over the measured wavelength ranges. It was also found that μ_s' highly depends on the wood species (μ_s' value differs between silver fir and sweet chestnut wood greatly). μ_s' of wet wood was significantly small compared to dried wood because the refractive index mismatch between the wood cell wall substance and water in the pores is much smaller than that between wood cell and air. D'Andrea et al. also evaluated the moisture content of wood using the μ_a and found a high relationship between moisture content and the μ_a at a specific wavelength [11]. Kienle et al. investigated the origin of scattering in wood by comparing the light propagation in the microstructure of silver fir measured experimentally to simulation modeled by MC method [12]. They determined μ_s' (wet wood: 1.79 mm^{-1}, dried wood: 6.68 mm^{-1}) due to tracheids by solving Maxwell's equation. They also determined μ_{s-iso}', which is the scattering coefficient due to all other scattering media (rough border between the lumen and wood cell substance, pits, ray cells), calculated by fitting measured light propagation to simulated data. The light scattering in wood is significantly complex as wood is a hygroscopic, heterogeneous, cellular, and anisotropic material. Although the wood samples were regarded as a homogenous material when the μ_s' values were estimated using TR spectroscopic method, in fact, the scattering properties highly depended on the wood species and fiber direction because the cellular structure, which caused multiple light reflections at the boundary between cell wall and air (water), significantly differs between wood species (i.e., hardwood has various cell arrangements like ring-porous, diffuse-porous, radial-porous, and figured-porous). Kitamura et al. tried to determine true μ_a and μ_s' values of wood cell wall substance itself in order to construct the robust calibrations wood properties by NIR spectroscopy [13]. They expected that the μ_a and μ_s' values of the cell wall substance are identical or similar between species because the density of wood cell wall itself is about 1.4–1.5 g cm^{-3} regardless of species (wood density depends on the ratio of pore and cell wall volume in wood). As the density of cell wall is identical between species, it is thought that the factor affecting the optical properties might be the concentration ratio of the three main polymers in the cell wall (cellulose, hemicellulose, and lignin). As there was no specific absorption band at the wavelength used in their study (846 nm) as shown by Hans et al. [14], it implied that the concentration ratio of the cellulose, hemicellulose, and lignin does not strongly affect μ_a. In order to decide the true optical parameters of wood cell wall, Douglas fir wood samples were immersed in hexane, toluene, or quinolone and saturated with them to minimize the multiple light reflections at the boundary between pore cell wall substance in wood. TR transmittance result of organic liquid saturated wood samples was fitted to the diffusion approximation equation to decide μ_a and μ_s'. μ_s' showed the minimum value when the wood was saturated with toluene because the refractive index of toluene is close to wood cell wall substance. In the toluene saturated wood sample, Fresnel reflection (1) at small particle, (2) between lumen and wood cell wall substance for all cell types (tracheid, ray cells, vessel), and (3) at the rough border are minimized because refractive index mismatch between toluene and cell wall was very small. The optical parameters of

wood cell wall substance calculated taking into account the volume fraction of wood cell wall substance were $\mu_a = 0.030\ \text{mm}^{-1}$ and $\mu_s' = 18.4\ \text{mm}^{-1}$. Konagaya et al. [15] fully investigated the effect of boundary between cell wall substance and air or water (refractive index mismatch) on the μ_s'. They investigated optical properties of drying wood with the moisture contents ranging from 10 to 200% by TR spectroscopy. They divided the source of light scattering into two factors, 1. scattering from large scatters (i.e., scattering diameter is much larger than the wavelength λ of the light), which can be described by geometric optics, expressing light propagation in terms of rays, and 2. scattering from small scatters (i.e., when the scattering diameter is the same as or less than λ), where Mie theory ($\approx\lambda$) or Rayleigh theory ($<\lambda$) is applicable. They revealed the contribution of scattering source at each stage of wood drying (constant rate, initial part of the first decreasing rate, later part, and second decreasing rate period). Scattering from dry pores dominated during the constant drying rate period, and the drying process of smaller pores dominated during the period of decreasing drying rate. The surface layer and interior of the wood exhibit different moisture states, which affect the scattering properties of the wood. The light propagation in wood complex cell structure is simulated by MC method taking into account the light reflection and transmission at the boundary between wood cell wall substance and pore by Ban et al. [16]. They investigated the relation of wood texture parameters calculated from cross-sectional microscopic images of the 13 species of wood samples and μ_s' at 846 nm. They found that μ_s' has linear relation to the air-dry density ($R^2 = 0.56$), quadratical relation to the cell–wall area ratio ($R^2 = 0.76$), and exponentially relation to the median pore area ($R^2 = 0.54$). 85 percent of the variation in μ_s' between many wood species can be explained by these three parameters. They simulated the light propagation in wood using the measured cross-sectional microscopic image of wood. After they performed segmentation of the microscopic image and recognized the pixel corresponding to cell wall substance and air area, the simulations were performed in the MC code, MCVM. The refractive index mismatch at the boundaries is also considered to improve the precision of simulations in MCVM code. Figure 11.2 shows simulated photon propagation in (a) agathis, (b) yellow poplar, and (c) rubber wood. It is observed that photon spreads farther in wood cell wall woods through continuously connected cell walls. The high correlation of cell–wall area ratio and median pore area on μ_s' can be attributed to the thicker, more connected cell walls associated with large cell–wall area ratio and small median pore area. Accordingly, increasing the area ratio of the cell wall and decreasing the pore area increased the μ_s'.

11.7 Brief Explanation for SR Spectroscopy

Not only the TR spectroscopy, some techniques are used to determine the optical properties. SR technique was developed to understand light propagation in turbid media. Compared to TR spectroscopy, SR technique is well suitable for use in post-harvest applications thanks to its low instrumentation cost, easy implementation.

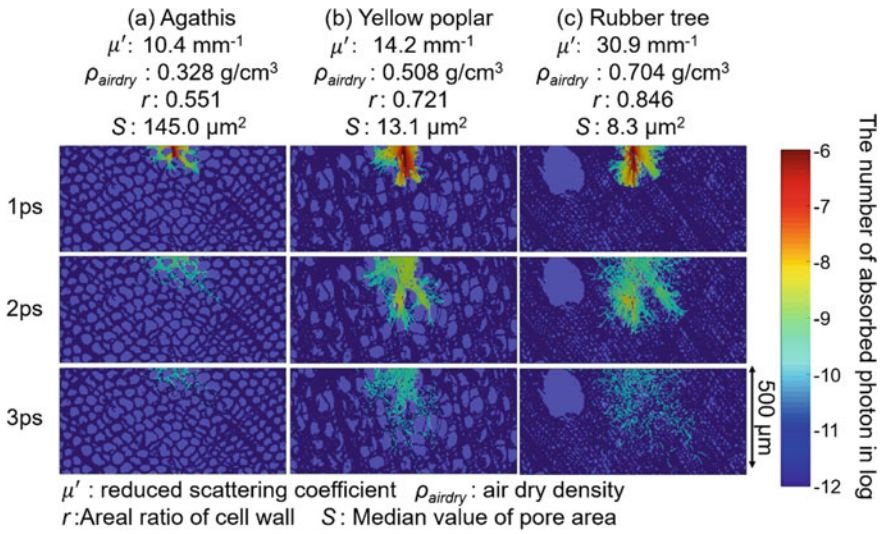

Fig. 11.2 Light propagation in **a** agathis, **b** yellow poplar, and **c** rubber wood simulated by the Monte Carlo method

For the SR technique, the point light source is generally injected on sample and the spatial distribution surrounding the injected light is detected by optical fiber arrays or non-contact reflectance image, which can be implemented with fiber optic probe, monochromatic imaging, and hyperspectral imaging. Measured spatial distributions were fitted by the analytical equation derived by Farrell et al. [17] with an appropriate inverse algorithm.

11.8 New Measurement System Minimizing the Effect of Light Scattering.

It can be extremely difficult to obtain reliable calibrations with highly scattering medium by conventional NIR spectrometer if both of the scattering and absorption properties of the samples vary. For example, variations of light scattering with size or concentration of rubber particles in latex samples are complicate. The variation of scattering properties in sample makes it difficult to interpret the quantitative analyses and to construct linear calibrations (multiple linear regression, principal component regression, and partial least squares regression). Shimomura et al. established three-fiber-based diffuse reflectance spectroscopy (TFDRS) based on spatially resolved spectroscopy to estimate the sugar content in fruits or total hemoglobin concentration and tissue oxygen saturation in human tissues using wavelengths range of 800 nm to 1100 nm [18–20]. A geometry of the TFDR spectrometer is shown in Fig. 11.3. A continuous wave laser beam is emitted into the sample through an optical fiber.

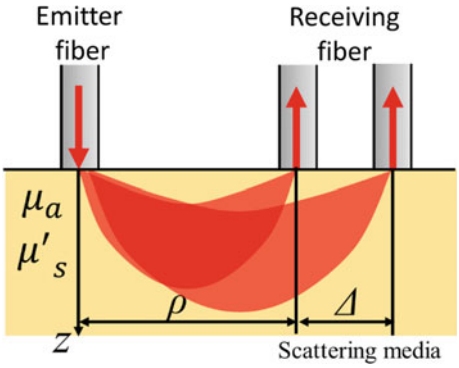

Fig. 11.3 Geometry of TFDRS

The spatially resolved light is collected by fibers that guide the light to the detector. The receiving fibers are aligned parallel to the distance of ρ and $\rho + \Delta$ apart from the emitting fiber. Shimomura et al. showed that a new physical parameter γ, which is calculated using the ratio of light intensity detected at distances ρ and $\rho + \Delta$, is independent of the optical path length and showed good linear relation to the analyte material concentration. One of the advantages of this method is that it is not necessary to measure reference signal. Shimomura et al. further developed a new system using three laser diodes at wavelengths of 911, 936, and 1055 nm, which were found as the best combination of wavelength to predict the sugar content of fruit. The sugar content in apples in the range of about 9–15 Brix was greatly predicted with high accuracy (Brix is an approximation of dissolved solid content in samples, representing the relation to a solution as a percentage of mass). They also constructed a small and cheap handheld commercial device employing NIR-LED and Si detector. Inagaki et al. showed this kind of technique using the wavelength range 850–1060 nm, which is a good method to decide the quality in highly scattering media, natural rubber latex samples [21]. They showed parameter γ has a strong linear relation to total solid content in latex (range 0.3–0.6 g g^{-1}) with a coefficient of determination value of 0.98 and root mean square error for total solid content of 0.014 g g^{-1}. Although the NIR spectra measured by conventional transmission or reflectance spectroscopy were highly affected by the scattering coefficient in the sample, simulation results in that study showed that the effects of scattering in the samples on γ can be reduced.

References

1. M.S. Patterson, B. Chance, B.C. Wilson, Time resolved reflectance and transmittance for the noninvasive measurement of tissue optical properties. Appl. Opt. **28**(12), 2331–2336 (1989)
2. L. Leonardi, D.H. Burns, Quantitative measurements in scattering media: photon time-of-flight analysis with analytical descriptors. Appl. Spectro. **53**(6), 628–636 (1999)

3. O.H.A. Nielsen, A.A. Subash, F.D. Nielsen, A.B. Dahl, J.L. Skytte, S. Andersson-Engels, D. Khoptyar, Spectral characterisation of dairy products using photon time-of-flight spectroscopy. J. Near Infrared Spec. **21**(5), 375–383 (2013)
4. A. Torricelli, D. Contini, A.D. Mora, E. Martinenghi, D. Tamborini, F. Villa, A. Tosi, L. Spinelli, Recent advances in time-resolved NIR spectroscopy for nondestructive assessment of fruit quality. Chem. Eng. Trans. **44**, 43–48 (2015)
5. R. Lu, R.V. Beers, W. Saeys, C. Li, H. Cen, Measurement of optical properties of fruits and vegetables: a review. Postharvest Biol. Tec. **159**, 111003 (2020)
6. H. Fujii, Y. Yamada, K. Kobayashi, M. Watanabe, Y. Hoshi, Modeling of light propagation in the human neck for diagnoses of thyroid cancers by diffuse optical tomography. Int. J. Numer. Meth. Bio. **33**(5), 1–12 (2017)
7. Y. Hoshi, Hemodynamic signals in fNIRS. Prog. Brain Res. **225**, 153–179 (2016)
8. F. Martelli, S.D. Bianco, A. Ismaelli, D. Zaccanti, Light propagation through biological tissue and other diffusive media.Theory, solutions, softw. (2009)
9. S.L. Jacques, Optical properties of biological tissues: a review. Phys. Med. Biol. **58**(11), R37–R61 (2013)
10. C. D'Andrea, A. Farina, D. Comelli, A. Pifferi, P. Taroni, G. Valentini, R. Cubeddu, L. Zoia, M. Orlandi, A. Kienle, Time-resolved optical spectroscopy of wood. Appl. Spectro. **62**(5), 569–574 (2008)
11. C. D'Andrea, A. Nevin, A. Farina, A. Bassi, R. Cubeddu, Assessment of variations in moisture content of wood using time-resolved diffuse optical spectroscopy. Appl. Opt. **48**(4), 87–93 (2009)
12. A. Kienle, C. D'Andrea, F. Foschum, P. Taroni, A. Pifferi, Light propagation in dry and wet softwood. Opt. Express **16**(13), 9895–9906 (2008)
13. R. Kitamura, T. Inagaki, S. Tsuchikawa, Determination of true optical absorption and scattering coefficient of wooden cell wall substance by time-of-flight near infrared spectroscopy. Opt. Express **24**(4), 3999–4009 (2016)
14. G. Hans, R. Kitamura, T. Inagaki, B. Leblon, S. Tsuchikawa, Assessment of variations in air-dry wood density using time-of-flight near-infrared spectroscopy. Wood Mater. Sci. Eng. **10**(1), 57–68 (2015)
15. K. Konagaya, T. Inagaki, R. Kitamura, S. Tsuchikawa, Optical properties of drying wood studied by time-resolved near-infrared spectroscopy. Opt. Express **24**(9), 9561–9573 (2016)
16. M. Ban, T. Inagaki, T. Ma, S. Tsuchikawa, Effect of cellular structure on the optical properties of wood. J. Near Infrared Spec. **26**(1), 53–60 (2018)
17. T.J. Farrell, M.S. Patterson, B. Wilson, A diffusion theory model of spatially resolved, steady-state diffuse reflectance for the noninvasive determination of tissue optical properties in vivo. Med. Phys. **19**(4), 879–888 (1992)
18. Y. Shimomura, S. Miki, T. Tajiri, H. Tanaka, Noninvasive measurement of absolute hemodynamic components in human tissue using three-fiber-based diffuse reflectance spectroscopy. in *2009 IEEE LEOS Annual Meeting Conference Proceedings* (2009), pp. 274–275
19. Y. Shimomura, T. Okada, Development of nondestructive measurement technique for fruits sugar content with near-infrared laser diodes operating at three different wavelengths. Rev. Laser Eng. **33**(9), 620–625 (2005)
20. Y. Shimomura, T. Takami, Y. Ichimaru, K. Matsuo, R. Hyodo, New measurement technique that uses three near infrared diode lasers for nondestructive evaluation of sugar content in fruits. Proc. SPIE 5739, Light-Emitting Diodes: Res. Manuf. Appl. IX **5739**, 145 (2005)
21. T. Inagaki, D. Nozawa, Y. Shimomura, S. Tsuchikawa, Three-fibre-based diffuse reflectance spectroscopy for estimation of total solid content in natural rubber latex. J. Near Infrared Spec. **24**(4), 327–335 (2016)